



LUND UNIVERSITY

Experimental and theoretical comparison of spatially resolved laser-induced incandescence signals in a sooting flame

Bladh, Henrik; Delhay, Jerome; Bouvier, Yoann; Therssen, Eric; Bengtsson, Per-Erik; Desgroux, Pascale

Published in:
Proceedings of the European Combustion Meeting

2005

[Link to publication](#)

Citation for published version (APA):

Bladh, H., Delhay, J., Bouvier, Y., Therssen, E., Bengtsson, P.-E., & Desgroux, P. (2005). Experimental and theoretical comparison of spatially resolved laser-induced incandescence signals in a sooting flame. In *Proceedings of the European Combustion Meeting*

Total number of authors:
6

General rights

Unless other specific re-use rights are stated the following general rights apply:
Copyright and moral rights for the publications made accessible in the public portal are retained by the authors and/or other copyright owners and it is a condition of accessing publications that users recognise and abide by the legal requirements associated with these rights.

- Users may download and print one copy of any publication from the public portal for the purpose of private study or research.
- You may not further distribute the material or use it for any profit-making activity or commercial gain
- You may freely distribute the URL identifying the publication in the public portal

Read more about Creative commons licenses: <https://creativecommons.org/licenses/>

Take down policy

If you believe that this document breaches copyright please contact us providing details, and we will remove access to the work immediately and investigate your claim.

LUND UNIVERSITY

PO Box 117
221 00 Lund
+46 46-222 00 00



LUND UNIVERSITY

Department of Physics

LUP

Lund University Publications

Institutional Repository of Lund University

Found at: <http://www.lu.se>

This is a camera-ready conference paper originally presented at
European Combustion Meeting, Louvain la Neuve, Belgium,
2005

This paper has not been peer-reviewed.

Citation for the published paper:

Author: Henrik Bladh, Jerome Delhay, Yoann Bouvier, Eric
Therssen, Per-Erik Bengtsson, Pascale Desgroux

Title: Experimental and theoretical comparison of spatially
resolved laser-induced incandescence signals in a sooting flame
Proceedings of the European Combustion Meeting, Louvain la
Neuve, Belgium, 2005

Official site for the European Combustion Meeting 2005:

<http://www.gfcombustion.asso.fr/index.php?langue=en&page=ecm.php&item=ecm>

Experimental and theoretical comparison of spatially resolved laser-induced incandescence signals in a sooting flame

H. Bladh², J. Delhay¹, Y. Bouvier¹, E. Therssen¹, P-E. Bengtsson², P. Desgroux¹

¹PC2A, UMR CNRS 8522/PC2A "Physico-Chimie des Processus de Combustion et de l'Atmosphère"
FR CERLA CNRS 2416 - Université des Sciences et Technologies de Lille

59655 Villeneuve d'Ascq Cedex – France

²Division of Combustion Physics, Lund Institute of Technology, P.O. Box 118, 221 00 Lund, Sweden

Abstract

A detailed experimental and theoretical investigation has been made on the use of Laser-Induced Incandescence (LII) in two configurations; right-angle LII and backward LII. Both right-angle and backward LII imaging measurements were conducted in simultaneous experiments at various pulse energies. The theoretically calculated LII signals were based on a heat transfer model for soot particles exposed to laser radiation, and were compared with the experimental LII images. Both the experimental and theoretical results from this initial comparison showed similar general behaviour, for example the broadening of the spatial LII distribution and the hole-burning effect at centre for increasing laser pulse energies.

1 Introduction

The laser-induced incandescence (LII) technique (based on the heating of soot particles followed by detection of the subsequent thermal radiation) has evolved as a powerful technique for quantitative measurements of soot volume fractions [1]. The relation between the LII signal and the soot volume fraction has been investigated in many studies both theoretically and experimentally. In the theoretical work by Melton [2], an expression was derived showing that for a sufficiently intense laser pulse the prompt LII signal was proportional to D^x where $x = 3 + 0.154/\lambda_{\text{det}}$ (D = particle diameter, λ_{det} = detection wavelength in μm). For detection wavelengths in the visible spectral range it means roughly a proportionality between the LII signal and soot volume fraction. This relationship has also been observed in several experimental investigations, mainly based on extinction measurements in well-characterised flames [3-5].

Still, however, fundamental knowledge of the processes underlying the LII signal behaviour is partly unknown. The models describing the heat and mass transfer between the laser radiation, the soot particles and the surrounding gas normally includes absorption of laser radiation, heat conduction, thermal radiation and sublimation, [6,7] but these terms include a large number of thermodynamic [8], physical and optical properties with large uncertainties in their values. Moreover, additional effects such as thermal annealing, photofragmentation and oxidation may not be negligible and might also, at least at some conditions, improve the models [9].

To improve LII as a quantitative tool for extraction of soot properties, the models describing the heat and mass transfer between the particles and the surrounding gas must be tested against well-characterized experiments. In this work, the laser-induced incandescence (LII) technique is applied in a sooting flame using an unfocused laser beam at 1064 nm. The distribution of the LII signal along the laser beam is

imaged using two directions of observation: one counter to the propagation direction of the incident laser (backward LII) and one perpendicular to the laser propagation direction (right-angle LII). It is shown that the LII probe volume is highly dependent on the laser irradiance and on its spatial distribution. At high fluence, the central part of the beam where the laser energy density is the highest exhibits an important decrease of the LII signal due to soot sublimation while a large widening of the LII cross-section area is observed. This recently observed phenomenon [10] has in this investigation been studied simultaneously using right-angle LII and backward LII, and the results have been compared with a recently developed heat and mass transfer model for soot particles probed using LII [11].

2 Experimental Arrangements

Experiments were performed in a sooting laminar diffusion flame stabilized on a McKenna burner (manufactured by Holthuis Inc.) equipped with a central injector as shown in Fig. 1. Different mixtures of fuels could be introduced through the injector allowing the stabilisation of a large range of diffusion jet flames surrounded by a flat flame of methane (C/O ratio = 0.8, $v = 12$ cm/s).

In this work we present results obtained in a laminar ($Re = 34$) methane diffusion flame ($Q = 100$ cm³/min., $v = 13.7$ cm/s). Perturbations from ambient air were minimized by a shielding air flow ($v = 73$ cm/s). A quartz collector located at 50 mm above the flat flame burner improved the flame stability. Measurements were performed 35 mm above the injector in a flame zone presenting a radial axi-symmetric soot distribution.

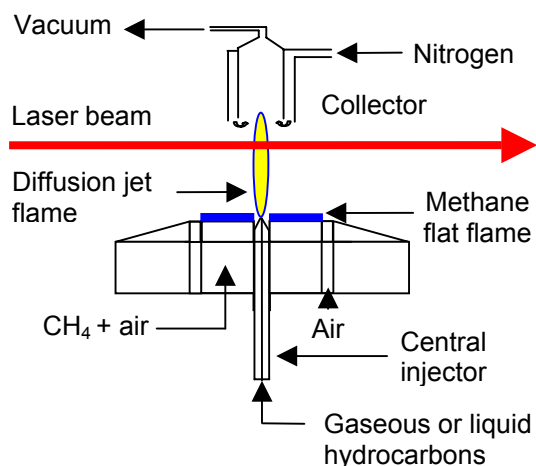


Figure 1. The experimental burner arrangement.

The experimental set-up is shown in Fig. 2. The laser is a Nd:YAG laser (Quantel Brilliant) operating at 1064 nm. Using a 1 mm diaphragm, the central part of the unfocussed near-Gaussian laser beam was selected and the beam propagated through the flame in the horizontal direction. The energy after the diaphragm was varied between 0.01 mJ and 8 mJ using the combination of a half-wave plate and a Glan prism.

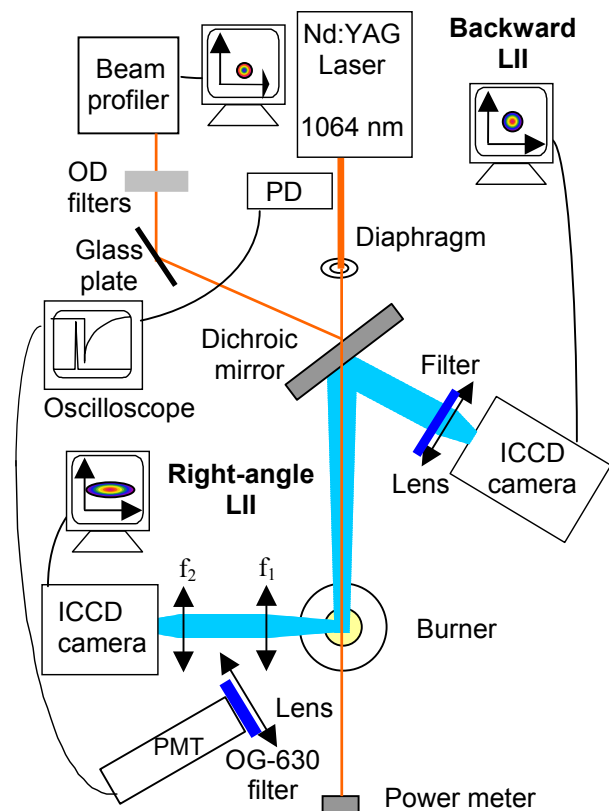


Figure 2: Experimental set-up. The burner is schematically represented (top view). PD: photodiode. PMT: photomultiplier tube.

The characteristics of the laser beam in terms of spatial distribution were monitored in the experiments using a CCD beam profiler (Gentec EO WinCamD). During the measurements a resolution of 9.4 microns was used in both the horizontal and vertical dimension. The faint laser beam reflection created by the entrance surface of the beam splitter (See Fig. 2) was led to a glass plate from which a second reflection was created. This reflection was aligned through a series of OD filters onto the CCD chip of the laser beam profiler. The amount of filter attenuation was adjusted when changing laser pulse energy to ensure a good dynamic range of the beam profile data. The distance from the profiler to the diaphragm was the same as from the flame to the diaphragm. Fig. 3 displays the spatial distribution of the laser beam energy transmitted by the diaphragm for a pulse energy of 2.0 mJ. The profile was recorded for all pulse energies used during measurements of LII. Analysis showed that the profile was almost independent of pulse energy.

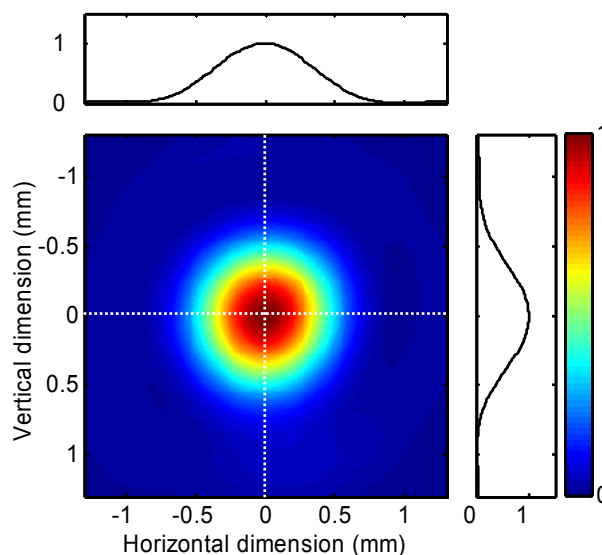


Figure 3. The spatial distribution of laser energy. The beam had a FWHM of ~ 0.83 mm. At the right is also shown the false colour scale used throughout this paper.

The sooting region of interest was imaged using two directions of observation: one perpendicular to the laser propagation direction (right-angle LII) leading to images of the spatial LII distribution along the beam, and the other one counter to the propagation direction of the incident laser (backward LII) leading to images of the spatial LII distribution in the cross section of the laser beam. The two configurations are illustrated in Fig. 4 together with examples of 2D-images, and a coordinate system that will be useful for the orientation of the presented images in figures presented later.

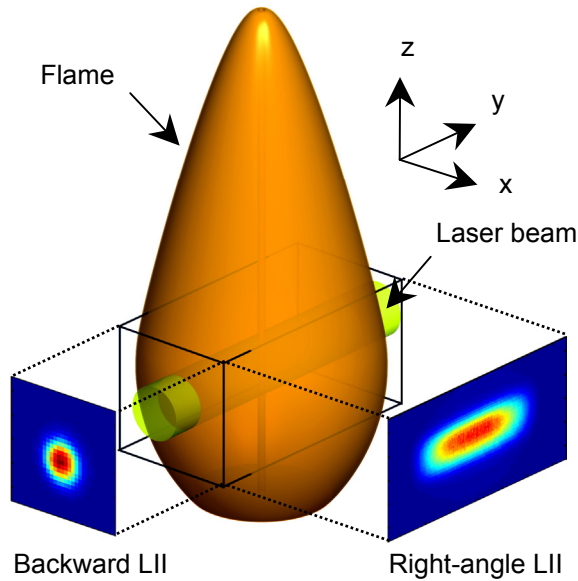


Figure 4. The two studied LII configurations (backward LII and right-angle LII) and their relation to the measurement volume.

In the backward LII configuration, incandescence was collected backwards within a solid angle of about $2.1 \cdot 10^{-5}$ steradians. The LII signal was reflected by a 10-cm diameter dichroic beam splitter, spectrally filtered between 400 and 700 nm and imaged on a 1280x1024 pixels ICCD Dicom Pro camera (pixel size = $6.7 \mu\text{m}$) using a 94 mm UV CERCO camera lens. The magnification was set to 13 (1 pixel in the image corresponds to $87.5 \mu\text{m}$ in the flame). A typical backward LII image has been inserted in Fig. 4.

With right-angle LII, the broadband LII signal was collected perpendicular to the laser propagation direction using a set of two doublets ($f_1 = 400 \text{ mm}$ and $f_2 = 200 \text{ mm}$) and imaged onto a ICCD Princeton camera with 384x576 pixels (pixel size = $22 \mu\text{m}$). A typical right-angle image has been inserted in Fig. 4. For this camera one pixel in the image corresponds to $44 \mu\text{m}$ in the flame. The soot distribution is axisymmetric relative to the y-axis, and can be considered as uniform within the small height (around 1 mm) illuminated by the laser beam along the z-axis.

The time-resolved LII signal was registered on a photomultiplier (PMT) and will be analysed later in terms of particle sizes.

3 Theoretical calculation of LII signal

The theoretical investigations presented in this paper have all been based on results obtained using a time-resolved heat and mass transfer model of one spherical

soot particle during its exposure to a laser pulse. This heat and mass transfer model is based on the one originally presented by Melton [2], and is described in detail elsewhere [10]. The experimental investigations have been performed using imaging techniques both from right-angle and backwards from the measurement volume and for the calculations a three-dimensional mesh of points was created covering this volume. The position of the mesh is indicated by the rectangular volume in Fig. 4. In every point (cell) the laser fluence and the soot volume fraction was defined. The laser fluence was directly given from the laser energy, the laser beam profile, and the mesh resolution, which was 9.4 microns along x and z, and 35 microns in the y-dimension. Since the flame was thin, absorption was considered negligible, and the spatial distribution of laser energy was considered constant along the beam propagation direction. The soot volume fraction was measured using right-angle LII and that data was given as input for the heat and mass transfer model. As input data for the model, the size of the primary soot particle has been set to 18 nm and the flame temperature to 1800 K. Since the beam was in the order of 1 mm in diameter and the flame $\sim 10 \text{ mm}$, soot volume fraction was considered uniform in the x-z plane. The heat and mass transfer model was used to predict the signal contribution from each cell in the mesh. The time-resolved signal curve was numerically integrated with the same gate timing as used during the experiments. The calculations resulted in a tensor of intensity values – one from each cell in the three-dimensional measurement volume. By summing the LII signal contributions in the laser propagation direction for backward LII, and along the x-axis for right-angle LII, theoretical LII signal images could be created that directly would correspond to the experimental images.

4 Results and Discussion

Two-dimensional images of spatial LII signal distributions are presented in Fig. 5 for both configurations (backward LII and right-angle LII) and in both cases from theoretical calculations as well as for experiments, for four different laser pulse energies. The false colour intensity represents the number of photons collected by each camera after flame emission subtraction. The backward LII images give the radial distribution of the LII signal spatially integrated along the y-axis (approximately 10 mm). The right-angle LII images are spatially integrated in the direction of observation i.e. in the x-direction (approximately 1 mm). The data sets have been obtained using a prompt LII signal and a gate width of 100 ns.

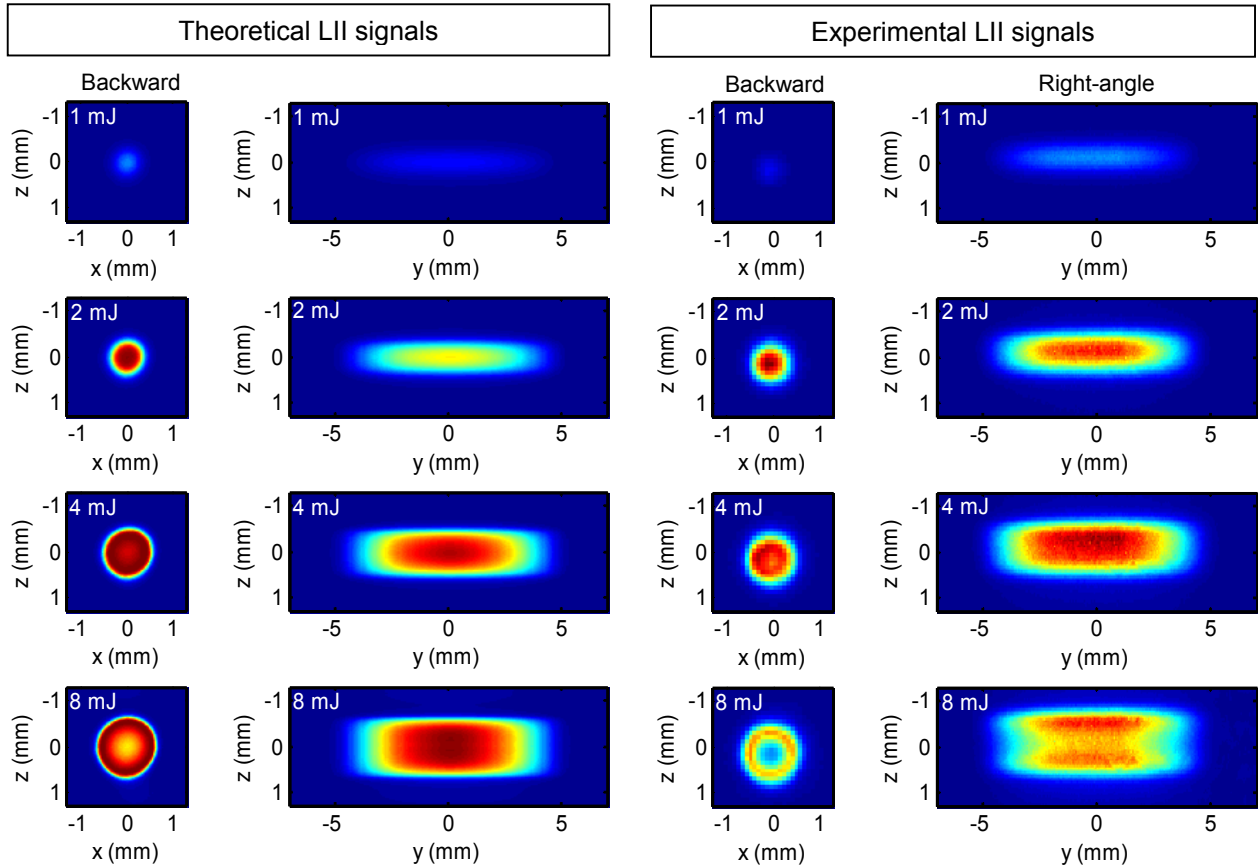


Figure 5. Theoretical and experimental LII signals using the two configurations. The images have been scaled relative to the highest intensity value among the images of each column.

When observing the experimental images in Fig. 5 it is clearly shown that (1) the spatial laser energy distribution widens for increasing energies and (2) a hole is formed at the centre of the beam. This hole-burning effect is obvious in both the images from backward LII and right-angle LII at 8 mJ. When comparing with the theoretical calculations (8 mJ), the hole-burning effect is clearly observable in the backward LII image but not in the right-angle LII image, which more shows a plateau.

The LII signal has been displayed versus laser pulse energy in Fig. 6. The theoretical curve has been derived by the model for one particle. In a real situation this shape would correspond to that obtained from a uniform distribution of equally sized soot particles heated by a laser pulse with a top-hat spatial distribution of laser energy. The experimental curve has been obtained by calculating the mean of nine close-lying pixels in the centre of the backward LII images. Since the spatial distribution of laser energy was changing very little with pulse energy, it is reasonable to assume that this curve can be treated as a result of uniform energy exposure. It can be noted that the threshold where the LII signal flattens out is relatively well predicted, whereas the experimental curve decreases faster than the theoretical one. This discrepancy at higher laser

energies explains why the hole-burning effect is more obvious in the experimentally recorded images.

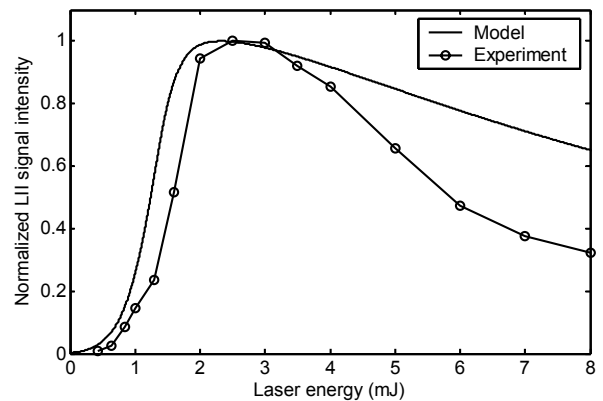


Figure 6. The normalized energy dependence of the LII signal from the centre part of the backward LII signal compared to the energy dependence predicted by the model for one particle.

In Fig. 7, the experimental and theoretical image profiles have been plotted for backward LII and right-angle LII for various laser pulse energies. Also in these profiles (1) the spatial widening of the LII signal distribution and (2) the hole-burning effect is shown for increasing laser pulse energies. In addition it can be

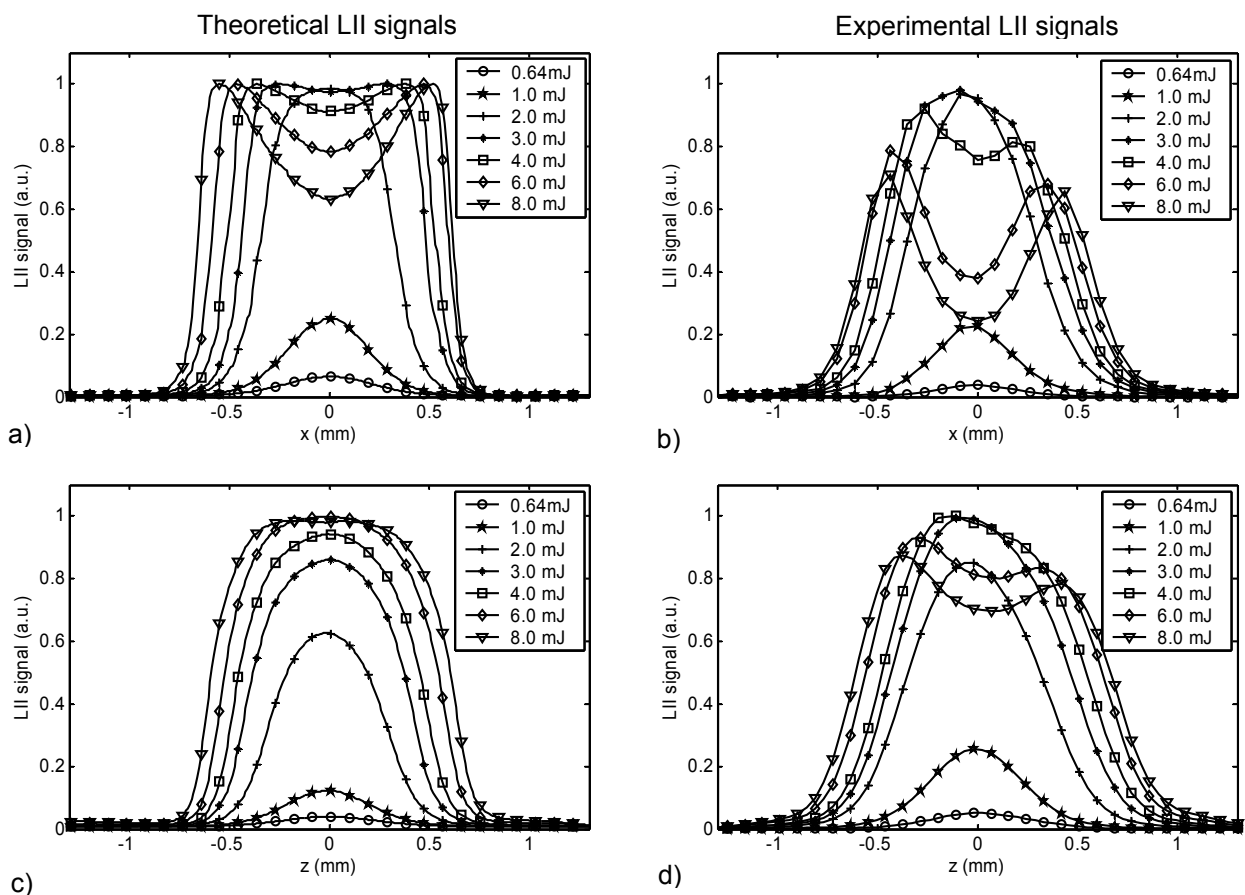


Figure 7. Experimental and theoretical LII signal profiles along the coordinate axis as a function of laser pulse energy. a) theoretical, backward LII, b) experimental, backward LII, c) theoretical, right-angle LII, d) experimental, right-angle LII.

observed that the experimental profiles have lower edges than the theoretical ones. One of the reasons for this is that the numerical spatial resolution is much higher than the experimental one. Thus a much improved comparison is expected when the experimental spatial resolution has been determined accurately and the profiles compensated. This lower spatial resolution is in fact obvious in the images in Fig. 5, especially in the experimental backward LII data.

There are a large number of parameters in the heat and mass transfer model that have uncertain values. It is thus important in the forthcoming treatment of the data to perform a sensitivity analysis in order to identify the major reasons for the presented discrepancies. One such parameter is the complex refractive index of soot. For example in this initial work we chose to treat the refractive index as independent of wavelength and the value $m = 1.57 - 0.56i$ was used in the model [12]. This would give the absorption function $E(m) = \text{Im}(m^2 - 1/m^2 + 2)$ the value 0.26. Other parameters that should be analysed in more detail are, for instance, filter transmission functions, thermodynamic parameters, the thermal accommodation factor, the assumed soot particle size, and the assumed flame temperature.

5 Summary

An extensive experimental investigation has been made to study the laser-induced incandescence (LII) signals from a well-controlled sooting flame. The LII signals were detected simultaneously in two configurations, backward LII and right-angle LII, using various pulse energies and various detector timings (delay, gate). The experimental work was supported by the theoretical calculations of LII-signals for both configurations, based on a heat and mass transfer model for single soot particles.

In this work the initial comparison of experimental and theoretical LII images has been made for a limited part of the measured data. For example, only one detector timing was chosen for the comparison, a prompt LII signal with a gate window of 100 ns.

The comparison between the experiments and the theoretical calculations is in general in good agreement regarding the general trends. Thus both the widening of the spatial LII distribution and the hole-burning effect for increasing pulse energies are found in both the experimental and the model data. However, there are parameters that have not been fully taken into account in the present model, and the experimental data set will be of high importance for improvements of the heat and mass transfer model for soot particles.

Acknowledgements

The authors would like to thank the European Commission for its financial contribution to this work within the AEROTEST project, contract N°AST3-CT-2004-502856, 6th PCRD, Auxitrol S.A. and MECAPA (Pôle capteur, FRED, FEDER, Conseil Régional Centre)

The CERLA (FR CNRS 2416) is supported by the French Research Ministry, by the Nord/Pas de Calais Region and by the European funds for Regional Economic Development. The authors thank the French Research Ministry under the contract D4P3 "Recherche Aéronautique sur le Supersonique",

The work by the Swedish research group was also financially supported by the Swedish Research Council.

References

1. Santoro, R.J. and C.R. Shaddix: Laser-Induced Incandescence. In: *Applied Combustion Diagnostics*, ed. by K. Kohse-Hoinghaus, J.B. Jeffries (Taylor and Francis, New York 2002) Chapt 9.
2. L.Y. Melton, *Appl. Opt.* **23**, No. 13, page 2201 (1984)
3. C.R. Shaddix, J. E. Harrington, and K. C. Smyth, *Combust. Flame* **99**, 723 (1994).
4. B. Quay, T. W. Lee, T. Ni, and R. J. Santoro: *Combust. Flame* **97**, 384 (1994)
5. P.-E. Bengtsson and M. Aldén, *Appl. Phys.* **B 60**, 51 (1995)
6. S. Will, S. Schraml, K. Bader, and A. Leipertz, *Appl. Opt.*, **37**, 5647 (1998)
7. G.J. Smallwood, D.R. Snelling, F. Liu, Ö.L. Gülder, *J. Heat Transfer*, 123, 814-818, (2001)
8. E. Therssen, C. Schoemaeker-Moreau, M. Carlier, C. Focsa, P. Desgroux,., submitted to *Carbon* (2005)
9. H.A. Michelsen, *J.Chem. Phys.* 118, 7012 (2003)
10. J. Delhay , Y. Bouvier, E. Therssen, J. D. Black, P. Desgroux, submitted to *Comb. Flame*
11. H. Bladh, P.E. Bengtsson, *Appl. Phys.B* **78**, 241 (2004)
12. K.C. Smyth, C.R. Shaddix, *Combust. Flame*, **107**, 314:320 (1996)